High-performance hybrid pervaporation membranes with superior hydrothermal and acid stability

Hessel L. Castricum [a,b,*], Robert Kreiter [c], Henk M. van Veen [c], Dave H.A. Blank [a], Jaap F. Vente [c], Johan E. ten Elshof [a]

[a] *Inorganic Materials Science, MESA+ Institute for Nanotechnology, University of Twente, P.O. Box 217, 7500 AE Enschede, The Netherlands*
[b] *Van't Hoff Institute for Molecular Sciences, University of Amsterdam, Nieuwe Achtergracht 166, 1018 WV Amsterdam, The Netherlands*
[c] *Energy research Centre of the Netherlands, Postbus 1, 1755 ZG Petten, The Netherlands*

ARTICLE INFO

ABSTRACT

A new organic–inorganic hybrid membrane has been prepared with exceptional performance in dewatering applications. The only precursor used in the sol–gel synthesis of the selective layer was organically linked 1,2-*bis*(triethoxysilyl)ethane (BTESE). The microporous structure of this layer enables selective molecular sieving of small molecules from larger ones. In the dehydration of *n*-butanol with 5% of water, the membrane shows a high separation factor of over 4000 and ultra-fast water transport at a rate of more than $20\,kg\,m^{-2}\,h^{-1}$ at $150\,°C$. This can be related to the high adsorption capacity of the material and the sub-micron thickness of the selective layer. The selectivity has now remained constant over almost one and a half years under continuous process testing conditions. Apart from the hydrothermal stability, the membrane exhibits a high tolerance for acid contamination. A slow performance decline in flux and separation factor is only observed at a pH lower than 2. The high stability and effective separation indicate a broad industrial application potential of the hybrid membrane material.

© 2008 Elsevier B.V. All rights reserved.

1. Introduction

Molecular separation with nanostructured membranes [1–9] can lead to substantial energy savings in the dehydration of biomass fuels [10] and of organic solvents [11–14]. The potential is similarly large in the dehydration of condensation reactions and in breaking azeotropic mixtures during distillation [15]. Typical examples are alcohol/water mixtures in which water is the minor component. The exergetic efficiency of conventional separation via distillation can be as low as 10% [16]. Economical industrial usage of molecular sieving membranes is however challenged by the development of a material that exhibits a favourable trade-off between selectivity and permeability and that at the same time performs with high stability and reliability under hydrothermal conditions. Membrane materials should withstand long-term operation at elevated temperatures, at least $150\,°C$, to resist the temperature of many process streams. High temperatures also bring about greater molecular mobility. This results in increased flux and reduces the required membrane surface area and hence the module costs. Long-term operation is required to minimise the high cost of membrane and/or module replacement and possible process discontinuation. Our assessments show that no substantial performance decline should occur within 2–3 years from the implementation of a module, which is in line with average maintenance intervals. While no amorphous material is truly stable, we here consider a membrane 'stable' when it can be applied under the desired operating conditions (*e.g.* high temperature) without the need for membrane replacement during this period.

Microporous amorphous silica materials on mesoporous ceramic supports are known to give effective dehydration membranes. The pore diameters of such membranes are typically between 2 and $4\,Å$, similar to the kinetic diameter of small molecules such as water (kinetic diameter $2.6\,Å$ [17]). Silica membranes combine a high permeability for small molecules with a very low permeability for larger ones ($>\sim 3\,Å$). They can be prepared by either chemical vapour deposition [18,19] or sol–gel hydrolysis and condensation [3,20]. However, inorganic silica is known to be hydrothermally unstable [21] which already becomes apparent at temperatures as low as $\sim 70\,°C$. Upon exposure to moisture, hydrolysis and net transport of silicon species lead to substantial loss of permeability within hours [22,23]. After prolonged

* Corresponding author at: Inorganic Materials Science, MESA+ Institute for Nanotechnology, University of Twente, P.O. Box 217, 7500 AE Enschede, The Netherlands. Tel.: +31 53 4892695/20 5256493; fax: +31 53 4893595/20 5255601.
E-mail addresses: H.L.Castricum@utwente.nl, H.L.Castricum@uva.nl (H.L. Castricum).

exposure to water, dense silica particles with associated large pores are formed, resulting in loss of selectivity. Membranes from other candidate materials, such as polymers and zeolites, have not yet provided an adequate combination of high permeability and stability. Polymers such as polyvinyl alcohol are structurally unstable above about 85 °C (its glass transition temperature) and do not withstand operation in various organic solvents [24,25]. The behaviour of ceramic-supported polyimide membranes is promising [26]. However, these polymers also have a limited lifetime of around 120 days at 150 °C under the harsh pervaporation conditions. Zeolites have excellent permselectivities, but it is challenging to grow them into ultrathin layers, while stability limitations exist as well [15,27].

Several approaches have been proposed for the improvement of the stability of amorphous ceramic membranes. One involves keeping coated membranes in humid air for a few days and calcining them in steam [28]. Another strategy is the application of pure metal oxides, which have more stable M–O bonds, such as amorphous TiO_2 or ZrO_2. However, these tend to crystallise in the presence of water even at low temperatures [29,30], thereby forming a discontinuous structure with substantially larger pores. Promising properties were found for a microporous $(Zr/Ti)O_2$ composite material, although the permselectivity for smaller molecules needs substantial improvement [31]. Another successful approach is the doping of silica with other inorganic oxides, including Al_2O_3, TiO_2, ZrO_2, MgO and Nb_2O_5 [32–34]. However, while this led to improved hydrothermal stability, the surface area and permeance were substantially reduced.

One of the most successful attempts to increase the hydrothermal stability to date has been the application of organically modified silica materials. These incorporate hydrolytically stable organic groups that are covalently bound to the silicon moieties. The introduction of methyl groups into the silica matrix has led to a substantial stability increase towards 95 °C [23]. This 'methylated' silica is prepared by co-condensation of tetraethylorthosilicate ($Si(OEt)_4$, TEOS) and methyltriethoxysilane (CH_3–$Si(OEt)_3$, MTES). The maximum concentration of alkyl groups that could be introduced was a CH_x:Si molar ratio of 0.5 [35,36]. The replacement of TEOS by 1,2-*bis*(triethoxysilyl)ethane ($(EtO)_3Si$–CH_2CH_2–$Si(OEt)_3$, BTESE) introduces organic bridges to the inorganic network structure, and the overall CH_x:Si molar ratio increases to 1. In this material, which was prepared by co-condensation of BTESE and MTES, the operating temperature towards dehydration was further increased to at least 150 °C [37,38]. The organic ethane links were suggested to inflict a greater toughness of the material, making it more resistant towards hydrolysis and cracking. The role of the methyl groups was supposed to provide additional shielding of the Si–O–Si bonds and prevent hydrolysis. The combination of BTESE and MTES thus resulted in a material with both high selectivity and hydrothermal stability. The material had very small micropores, making it selective in the dehydration of *n*-butanol, with a flux of up to $10 \, kg \, m^{-2} \, h^{-1}$ at 150 °C. Bridged precursors such as BTESE were originally introduced by Loy and Shea [39–41] and find extensive use in the preparation of periodic mesoporous organosilicas (PMOs) [42–44] using a variety of templates. However, as PMOs have mesopores >2 nm they have no molecular sieving properties. The microporous membrane material was prepared without a template and required sol–gel engineering with a limited number of reactants. Despite the presence of many non-polar organic groups, water transport through the membrane was substantial.

In the present work, we report the preparation of selective dehydration membranes by sol–gel condensation of BTESE only. It is the first molecular sieving membrane that is synthesised using one single bridged organosilane precursor. The recipe is a substantial simplification as compared to the previously reported recipe that

also included MTES. The much easier and more straightforward processing procedure opens up new ways to further develop and tailor this class of membrane materials. We describe the various processing stages that resulted in the preparation of defect-free selective membrane layers. These include engineering of the sol colloid structure, characterisation of the microporous solid structure with different molecular probes, and membrane testing. We investigated the flux of this material as compared to the previously reported hybrid membrane and show the dehydration ability towards *n*-butanol. We studied the acid stability of the material as well as the long-term stability in neutral conditions at elevated temperature (150 °C), which can be considered as essential assets for successful application in industrial separation processes.

2. Experimental

2.1. Material preparation

To remove any traces of impurities and water, 1,2-*bis*(triethoxysilyl)ethane (purity 96%, Aldrich) was distilled at reduced pressure before use. It was subsequently diluted with dry ethanol in an ice bath. Distilled water and nitric acid (65 wt%, Aldrich) were mixed and added drop-wise to the diluted precursor under vigorous stirring. The sol was then heated to 60 °C during 3 h under continuous stirring. In Table 1, silane concentrations, acid-to-Si ratio and hydrolysis ratio are compared to a previously reported membrane recipe **3** prepared from a mixture of BTESE and MTES [38]. A sol **2** with a lower silane concentration was prepared to enable membrane coating with a more dilute sol than **1**. Unsupported films were obtained by drying the sols in a Petri dish.

Supported mesoporous γ-alumina membranes were prepared by a dip-coating procedure of a boehmite sol on a 30-cm long tubular α-alumina support system (ID/OD = 8/14 mm, 40 cm², obtained commercially from TAMI) [45,46]. The freshly prepared hybrid sol was coated onto this γ-Al_2O_3 layer. Coating procedures were carried out under class 1000 clean room conditions to minimise defect formation due to dust particles. All layers were applied on the outside of the tubes. The supported and unsupported films were consolidated by a thermal treatment at 300 °C for 2 h in a nitrogen flow (99.999% pure), applying heating and cooling rates of 0.5 °C/min. The supported membranes were sealed with stainless-steel caps [47].

2.2. Characterisation of hybrid colloids, unsupported and supported films

Colloid sizes in the freshly prepared sols were determined by dynamic light scattering (DLS). The sols were diluted with three volume parts of EtOH and their colloid size was measured at 25 °C using a Malvern Zetasizer Nano ZS.

Small-angle X-ray scattering (SAXS) measurements were carried out at the DUBBLE beamline BM-26B [48] of the European Synchrotron Radiation Facility in Grenoble, France. Scattering data were obtained at an X-ray beam energy of 12 keV. The fractal

Table 1
Preparation parameters for sol recipes **1**, **2** and **3**: silane, nitric acid and water concentration

Sol recipe	[silane]ᵃ (mol l⁻¹)	[H⁺]:[Si]	[H₂O]:[Si]
1	0.75	0.08	2.7
2	0.45	0.10	3
3	1.2	0.067	3

ᵃ For **1** and **2** only BTESE was used; for **3**, a mixture of BTESE and MTES was used with a molar ratio of 1:1 and half of the water was added after 90 min.

dimension D_f was determined after background subtraction from an exponential fit of the intensity $I \sim e^{-D_f}$. Sol characterisation was found to be well reproducible.

Adsorption/desorption isotherms were obtained for dried ($p < 10^{-4}$ mbar at 473 K) thermally consolidated unsupported films on a CE-Instruments Milestone 200. N_2 isotherms were obtained at 77 K, and CO_2 and C_2H_2 isotherms at 273 K. From the adsorption isotherms, surface areas were determined by the Dubinin method, modified by Kaganer [49,50], represented by

$$\log n = \log n_m + D \left(\log \frac{p^0}{p} \right)^2$$

with n the gas adsorbed at relative pressure p/p^0, n_m the monolayer capacity of the surface, both expressed in mol per g adsorbent, and D an adsorbate-dependent constant. This constant has smaller (more negative) value for smaller pore sizes, and may serve as a check for the actual pore size assessment. Surface areas A were subsequently determined according to

$$A = n_m a_m N_A$$

in which N_A is Avogadro's number and a_m the area occupied by a molecule in the completed monolayer, taken as 0.162 nm^2 for N_2 (ISO 9277), 0.179 nm^2 for CO_2 and 0.204 nm^2 for C_2H_2. The error in the surface area, based on the difference with the blank isotherm, is about 5%. Reproducibility was much better than this error. The solid skeletal (network) density was determined by gas pycnometry at room temperature, with He as a replacement gas, in a Multivolume Pycnometer 1305 after the same drying procedure.

High-resolution scanning electron microscopy was carried out on a Jeol 6330F SEM equipped with a Noran Voyager EDX at a voltage of 5.0 kV.

Permporometry of a supported hybrid membrane was carried out with water vapour as the condensable gas and He as the diffusional gas [51,52], applying a drying temperature of 200 °C and a measurement temperature of 40 °C. By the application of a pressure gradient, helium transport occurred by a combination of molecular diffusion and pressure-driven transport. Pore size distributions were assessed using the Kelvin equation.

2.3. Membrane performance

Pervaporation of water from n-butanol was carried out using the supported membranes in a stirred vessel at 95 °C (95/5 wt% n-butanol/water, 1 bar) within days after membrane preparation. While we are currently defining the broader application window, we have selected the separation of water from n-butanol as a standard to compare the performances of our membranes. Water was continuously added with a pump to correct for the losses caused by the pervaporation process. Prolonged pervaporation with various concentrations of nitric acid was also carried out under these conditions. Nitric acid was added manually at regular intervals to keep the acid concentration at a stable value. Long-term pervaporation measurements were carried out under hydrothermal conditions for a membrane with a surface area of ~40 cm^2. Pervaporation was performed at 150 °C in a continuous flow set-up (5 bar). The feed was pumped with a constant flow of 1000 l/h from a 50-l storage vessel over six membrane modules that were aligned in series. The retentate was fed back to the feed vessel. A detailed description and scheme of the continuous-flow set-up are given elsewhere [26]. The performance of the membranes was determined individually at regular intervals with a feed mixture containing 2.5 wt% demineralised water in n-butanol (Merck P.A.). The permeate sides of all membranes was kept at 10 mbar with a vacuum pump. The compositions of the feed and the permeate were determined by Karl

Fischer titrations. For reasons of comparison the water fluxes are presented here according to a water content of 5 wt% in the feed. The separation factor, α, is defined as

$$\alpha = \frac{Y_w/Y_b}{X_w/X_b}$$

where Y and X are the weight fractions of water (w) and n-butanol (b) in the permeate and feed solutions, respectively.

3. Results

3.1. Sol preparation

We recently reported highly promising results for membranes based on mixtures of BTESE and MTES [37]. Because of the differences in gelation rates, these hybrid membranes were prepared using quite different reaction parameters than for standard inorganic silica membranes. We found that the viability of membrane synthesis is strongly related to the mean colloid size during coating of the selective layer [38]. The presence of MTES in the original recipe moderated the gelation rate. In an alternative approach, when BTESE is used as the only silane precursor, lower concentrations of the reactants (silane, water and acid) are required. MTES had been added as well to minimise auto-condensation and thus to prevent cyclisation reactions [41]. However, considering the strong dependency on a suitable colloid size distribution, we ignored the effect of possible cyclisation reactions in the present study. Instead, we focused on preparing sols with similar sol colloid sizes as those for a BTESE/MTES mixture that was reported earlier to give selective hybrid membranes [38]. We also attempted to avoid using a multi-step synthesis procedure, as we had found that this may lead to a discontinuous development of the sol colloidal structure [53]. Instead, we optimised the recipes in such a way that all reactants could be added in one step.

We investigated two different sol recipes **1** and **2** in detail using only BTESE. The sol colloid size distributions for the different recipes are shown in Fig. 1 and their mean colloid sizes are given in Table 2. The mean colloid size of recipe **1** is close to that of the earlier reported BTESE/MTES recipe **3** from which a selective and highly stable membrane was prepared. In order to reduce layer thickness and thus enhance permeability, sol **2** was prepared with a decreased silane concentration. The lower silane concentration led to a lower condensation rate and consequently to smaller colloids (3.3 nm) than for the sols **1** and **3**. Still, the colloids were notably
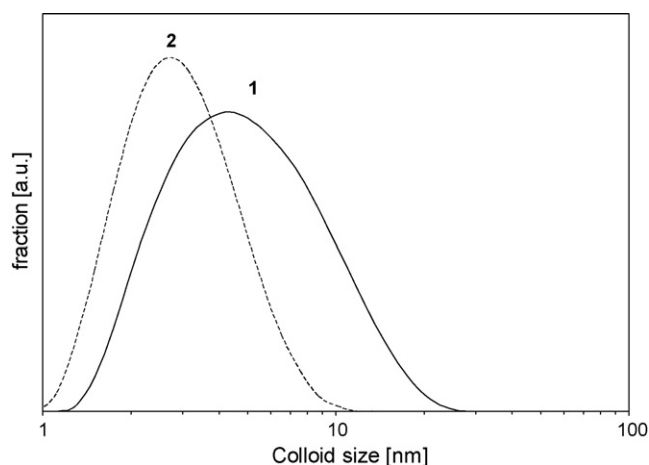

Fig. 1. Sol colloid size distributions of sol **1** (solid) and **2** (dashed), determined by dynamic light scattering.

Table 2
Colloid size and colloidal fractal dimension of BTESE-based sols **1** and **2**, compared to a reference material containing both BTESE and MTES (sol **3**)

Recipe	Mean sol colloid size (nm)	Fractal dimension
1	5.7	1.4
2	3.3	1.2
3	4.9	1.1

Table 3
Surface areas determined from adsorption isotherms with various molecular probes, the absolute value of the D parameter from the Dubinin fit of the CO_2 isotherm, and skeletal densities determined with He pycnometry

Recipe	Surface area A (m²/g)[a]			$|D|$	Density
	N_2	CO_2	C_2H_2	CO_2	He (g/ml)
1 (BTESE)	131	451	546	0.178	1.7
2 (BTESE)	311	422	514	0.176	1.7
3 (BTESE/MTES) [38]	0	344	1340	0.204	1.5

[a] The error in the surface area is about 5% while 'zero' surface area indicates $A < 10 \, m^2/g$.

larger than those of a BTESE/MTES mixture (2.2 nm) that had earlier been found to result in unselective thin layers [38].

To investigate the ability of the sols to form microporous structures, the fractal dimension D_f was measured by means of small angle X-ray scattering. This value is a measure of the degree to which the sol colloidal particles have a branched polymeric structure. Acid-catalysed condensation is known to result in colloidal particles that are constituted of polymeric chains with limited branching. For particles that have $D_f < 1.5$, these polymer chains can interpenetrate upon drying, resulting in a fully microporous material [54,55]. Colloids with fractal dimension larger than 1.5 would rather result in mesoporous structures due to 'hard sphere packing'. Such structures have pores in the order of the colloid size. Sol particles with a maximum D_f of 1.5 are thus required to obtain a network with a percolative structure and (sub)nanometer-sized pores. As the investigated sols had fractal dimensions below this maximum value (Table 2), they were both expected to form microporous solid materials upon drying. Interestingly, the fractal dimensions of the pure BTESE-based sols (**1** and **2**) are larger than that of the BTESE/MTES reference sol (**3**). This is even the case for sol **2**, which has a smaller colloid size than **3**. The internal structure of the BTESE molecule, which already consists of a bridging group with six reactive sites, is likely responsible for the apparent higher degree of branching.

3.2. Structure of solid gel

Solid unsupported films were prepared by drying the sols in a Petri dish. The films that were formed after solvent evaporation were structurally consolidated by a heat treatment at 300 °C identical to that of the membranes. The pore structure of unsupported gel **1** was investigated by vapour adsorption with N_2, CO_2 and C_2H_2. In this way, we could compare the adsorption isotherms of BTESE-based film **1** and **2** to that of film **3** made from BTESE/MTES (Fig. 2).
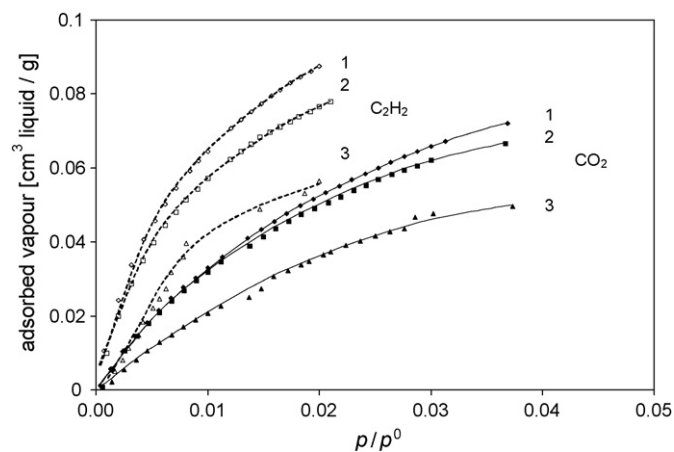

Fig. 2. Adsorption isotherms of CO_2 (closed symbols) and C_2H_2 (open symbols) of a thermally treated gel prepared from recipe **1** (diamonds) and **2** (squares), compared to isotherms of a BTESE/MTES-based gel **3** (triangles), expressed in volume of condensed (liquid) adsorbate.

Surface areas were calculated by a Dubinin fit for microporous materials (Table 3).

It is clear that more C_2H_2 than CO_2 is adsorbed on both BTESE-based hybrid materials (Fig. 2). This is in correspondence to what can be expected from the critical diameter of the different probe molecules. As C_2H_2 molecules can be transported through narrower pores, its adsorbance is higher for ultramicroporous materials (pore diameter <0.6 nm [56]). Similarly, a larger amount of CO_2 and C_2H_2 vapour was adsorbed on materials prepared from pure BTESE than on those from BTESE/MTES copolymers (Fig. 2). This indicates that a more open structure was formed by leaving out MTES during preparation. In addition, the differences in surface area, as determined from a fit of the CO_2 and C_2H_2 isotherms, were small. Considering the critical diameters [57] of the CO_2 (0.28 nm) and C_2H_2 (0.24 nm) molecules, this indicates a larger mean pore diameter in BTESE-based materials. This is also consistent with the smaller absolute value of the D parameter of the Dubinin fit of the CO_2 isotherm of **1**.

In contrast to the BTESE/MTES copolymer, which showed zero N_2 adsorption [38], the BTESE-based materials were found to be more open towards N_2 (the largest investigated molecular probe, critical diameter 0.30 nm). This is another indication that larger pores were formed in the BTESE-based materials without MTES. Adsorption of N_2 followed a type I isotherm, confirming that the material is microporous. Equilibration was slow, which is also apparent from lack of overlap of the desorption and adsorption branches. Slow equilibration is also the likely cause of the differences in the calculated surface area between **1** and **2**. Considering the smaller surface area for N_2 adsorption than for CO_2 and C_2H_2 and the slow equilibration of N_2 adsorption, it can be concluded that most pores are close to 0.3-nm wide in the unsupported BTESE-based material and smaller in the BTESE/MTES copolymer.

The skeletal network density of the materials was determined with He pycnometry. The values were well reproducible, with an error in the order of 0.02 g/cm³. As the materials have the same gross organic fraction, they would be expected to have similar skeletal densities, but a higher density was determined for BTESE-based hybrid silica than for BTESE/MTES-based silica. A higher network density indicates a smaller volume inaccessible to He and thus a smaller contribution to the total volume of closed (inaccessible) porosity. A similar effect was observed in materials from TEOS/MTES mixtures [58]. While the total pore volume increased with MTES concentration, this could mostly be attributed to very small pores. A substantial volume of the MTES-modified material appeared to be inaccessible for all molecular probes, and the presence of a large number of closed pores or regions with sizes below 0.2 nm was concluded [58]. The higher network density of BTESE-based materials compared to BTESE/MTES copolymers thus confirms the higher adsorption capacity. Although the structure of an unsupported film may differ from that of a membrane, the trends can usually be well found back in a supported system. Below, we will show that the increased adsorption capacity of a pure BTESE-
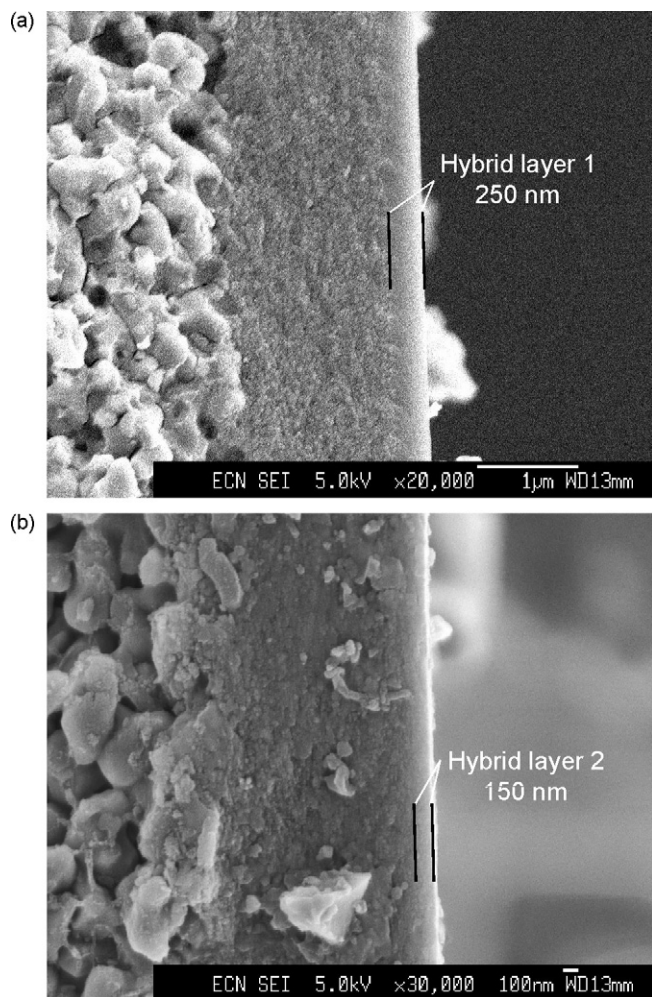
Fig. 3. Cross-sectional SEM micrographs of the layered structure of hybrid membranes prepared from sol **1** (a) and **2** (b), showing the supporting layers and the selective hybrid silica top layer. The hybrid top layers are indicated and have thicknesses of 250 and 150 nm, respectively.

based material indeed works out advantageously in membranes, despite the slightly larger pore size.

3.3. Membrane performance

Tubular membranes were prepared by a dip-coating procedure in a class 1000 clean room. We deposited thin films from the sols **1** and **2** on mesoporous γ-alumina tubular support systems with average pore diameters of around 4 nm. Inspection with an optical microscope showed that continuous and crack-free surfaces were formed after deposition and subsequent thermal treatment. SEM cross-sectional images (Fig. 3) show that the thicknesses of the top layers was 250 and 150 nm for the membranes made with sols **1** and **2**, respectively. The room temperature helium permeances of the freshly prepared membranes were indicative for a very small defect concentration.

The Kelvin pore size distribution of the microporous top layer of the membranes was estimated by means of permporometry. Water was applied as the condensable vapour and He as the diffusional gas. Water vapour and the vapours of non-polar compounds are all suitable for estimating pore size distributions [51]. In contrast to conventional permporometry with non-polar condensable vapours such as cyclohexane, pores smaller than 1 nm can also be observed by using water vapour. Condensed water was used
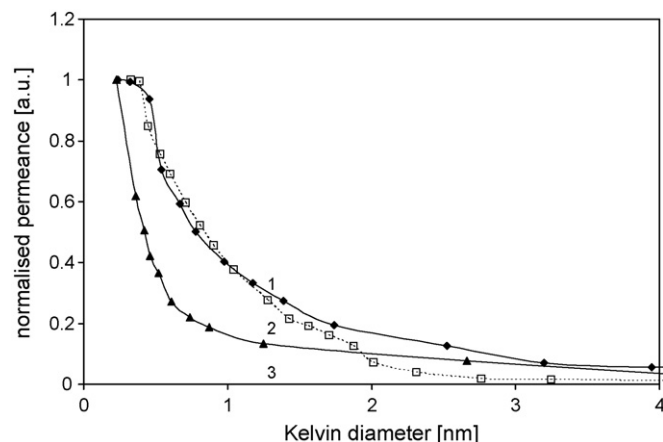

Fig. 4. Kelvin pore size distribution for hybrid membranes from sol **1** (diamonds) and **2** (squares) compared to BTESE/MTES-based membrane **3** (triangles).

to block all membrane pores up to a certain diameter, while He passed through the larger open pores. We established that the top layers were microporous and that the number of defects is very small, considering the very low (residual) permeance at high Kelvin diameters (Fig. 4). We found similar Kelvin pore size distributions of the two membranes **1** and **2**, with an average pore diameter (Kelvin diameter at 50% of the maximum He permeance) of 0.78 and 0.84 nm, respectively. This is in agreement with the adsorption data on unsupported thin films that were reported in the previous section. The pores had somewhat larger diameters than those of membrane **3**, prepared from a BTESE/MTES mixture [38], which showed an average pore diameter of 0.40 nm. These estimated values are somewhat larger than those measured with adsorption techniques. This can be attributed both to differences in the drying behaviour of the supported membranes as compared to that of the unsupported films, as well as to the intrinsic uncertainty in the precise value of using the Kelvin equation for pore diameters below 2 nm. However, the differences in porosity between the 2 types of material are clear and in full agreement with the larger pore sizes of the unsupported BTESE-based films.

Selective dehydration by pervaporation of *n*-butanol was carried out using a membrane from recipe **1** and **2** at 95 °C. Results obtained after 1 week of continuous pervaporation using a feed mixture containing 5 wt% water in *n*-butanol are shown in Table 4. This waiting period enables a more precise comparison, as initial fluxes are usually somewhat higher and separation factors lower. Membrane **2** was less selective than membrane **1**. However, the flux of **2** is much higher. This can be related to the smaller thickness of the selective layer, which results in less resistance. Interestingly, despite the larger mean pore size of these membranes, the separation factor was slightly higher than that of membrane **3**. This suggests that for this separation, the pores of the material are still sufficiently small to enable selective dehydration. In order to assess full applicability, we therefore focused our attention further on other relevant factors, *i.e.* optimisation of flux and stability.

Table 4
Water content of permeate and water flux after 7 days of continuous membrane operation in 95/5 wt% *n*-butanol/water pervaporation (95 °C)

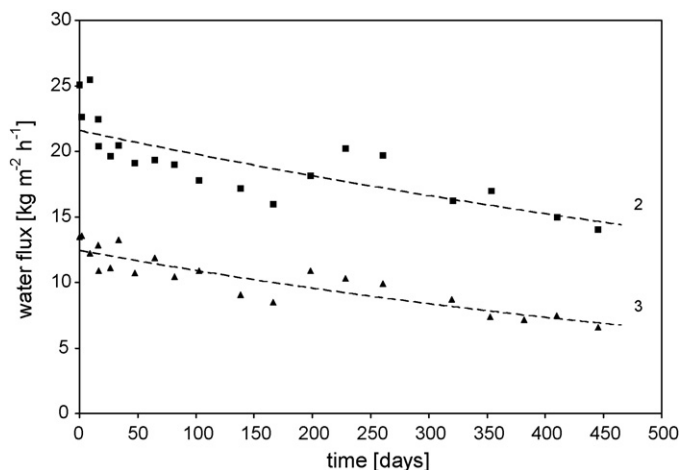| Membrane	Precursor	Water content in permeate (wt%)	Water flux ($kg\,m^{-2}\,h^{-1}$)
1	BTESE	99.3	3.3
2	BTESE	95	6.2
3	BTESE/MTES	92.2	2.0

Fig. 5. Long-term separation permeability of hybrid silica membranes from recipe **2** (squares) and **3** (triangles) towards dehydration of *n*-butanol (calculated for 5 wt% water in *n*-butanol) at 150 °C. The lines represent exponential fits of flux decline.

Fig. 6. Permeate water concentrations (a) and separation factor (b) of hybrid silica membranes from recipe **2** (squares) and **3** (triangles) during long-term dehydration of 2.5 wt% water from *n*-butanol at 150 °C.

Considering the high permeability of membrane **2**, this was selected for a long-term pervaporation experiment at 150 °C. A feed containing 2.5 wt% water in *n*-butanol was used. As a linear relation exists between the water flux and water concentrations in the range 1–10 wt%, all values were calculated to dehydration of a 95/5 wt% *n*-butanol/water mixture. This allows for direct comparison of this hybrid silica membrane to membrane **3** and with earlier data that were reported on that membrane in a stirred autoclave [38]. We found an initial steady-state water flux higher than 20 kg m^{-2} h^{-1} (Fig. 5), which decreased only very gradually. The water concentration in the permeate increased to >99 wt% (Fig. 6a), and to a separation factor of over ~4000 within the first 50 days of operation. This has remained unaltered during almost one and a half year. The performance was found to be reproducible with another membrane from the same material. The steady-state permeate water concentration is higher than that measured at 95 °C after 1 week, which is a very common observation for such membranes. The membrane is still under operation and highly selective at the time of submission. Earlier silica-based membrane generations exhibited rapid deterioration. Conventional silica and methylated silica break down within days at 95 and 115 °C, respectively [23]. The water flux of membrane **2** is a factor of 2 higher than that of BTESE/MTES-based membrane **3**, which had already shown the highest stable flux ever at this temperature. The membrane thus combines a spectacularly high separation factor and flux with the ability to function without substantial performance decline over more than one year at high temperature, *i.e.* 150 °C. This implies that economical dehydration of higher alcohols is well within reach, opening the way for implementation of membranes in large-scale industrial processes.

The open structure of the material and small layer thickness of this membrane are the main reasons for its unprecedented high flux. The flux through BTESE membrane **2** appears to be more consistent over time than for the BTESE/MTES hybrid **3**. The half-life of the flux is about 500 days for **3**, while it is 800 days for **2**. Interestingly, the long-term measurements on these membranes were performed in a continuous flow setup and reproduce the findings obtained with a stirred autoclave for membrane **3** [38]. Despite the differences in flow conditions at the membrane surface, this does not lead to a different profile of the water flux curve as a function of time. The slower flux decline for BTESE-based silica can likely be ascribed to an intrinsic property of the material, *i.e.* the absence of MTES in the recipe. As this moiety forms only three bonds with the silica network, complete hydrolysis of the ≡SiMe groups is more
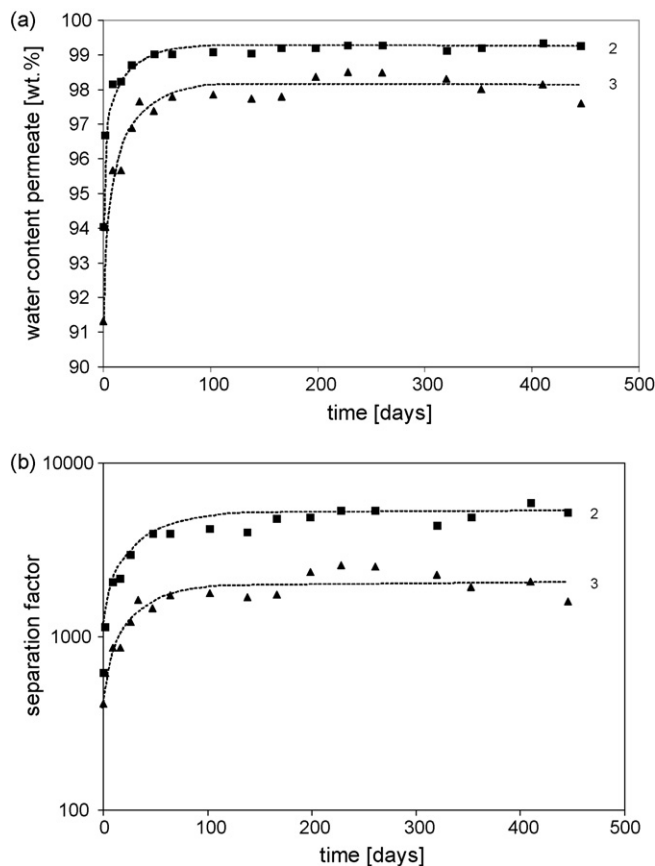
likely than hydrolysis of the ≡SiCH$_2$CH$_2$Si≡ moieties. As a result the diffusion of ≡SiMe fragments can lead to reorganization of the hybrid silica network, eventually causing a faster densification of the material and thus a faster decline of the flux. The current material is therefore an improvement of the previous one in more than one respect: not only is the recipe simpler and the obtained permeance higher, it also shows a higher flux-stability at 150 °C than any dehydration membrane reported before. The slow flux decline can possibly be related to loss of transport-enabling micropores under the severe hydrothermal conditions.

As several process streams to be dehydrated have a high acid concentration, *e.g.* from esterification reactions, we assessed the stability of the current material under such conditions. To this end, we studied the selectivity and permeance through membrane **1** at different acid concentrations, starting at the lowest. The tests were carried out at 95 °C. As this membrane was somewhat thicker than the one that was tested under neutral conditions, it exhibited a lower flux of initially 2.2 kg m^{-2} h^{-1}. No decline of membrane performance was found for HNO$_3$ concentrations of 0.005 and 0.05 wt% (Fig. 7). Only at a concentration of 0.5 wt% HNO$_3$ (0.04 M), which corresponds to a pH of 1.4 in aqueous solutions, a gradual decrease of permeate water concentration was observed, which is accompanied by a decline in water flux and slight increase in *n*-butanol flux. This suggests that loss of porosity and a re-organisation of the structure are initiated by exposure to a highly acidic mixture. Loss of porosity may lead to mechanical stresses, which also lead to the formation of larger defects, causing loss of selectivity. The performance decline upon prolonged exposure to a highly acidic feed eventually leads to membrane failure after 126 days. Still, the mem-
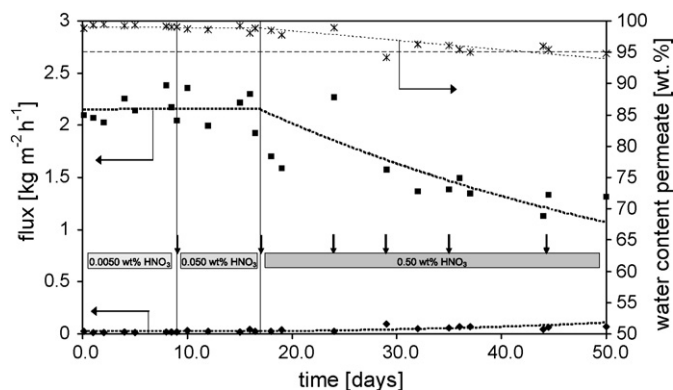
Fig. 7. Long-term separation performance (stars: water content of permeate; squares: water flux; diamonds: *n*-butanol flux) of a hybrid silica membrane from recipe **1** towards dehydration of *n*-butanol (calculated for 5 wt% water) at various acid concentrations and 95 °C. Vertical arrows indicate the times at which additional HNO₃ was added to keep the acid concentration constant. The dashed lines serve as a guide to the eye.

brane was found to be highly stable at lower acid concentrations (equivalent to pH ≥ 2), which is in correspondence to the substantial acid stability observed in unsupported BTESE/MTES materials [38].

4. Conclusions

A hybrid high-performance dehydration membrane has been prepared that allows extremely high flux and has a very high separation factor in the separation of water from *n*-butanol. The material consists of organically bridged silica moieties and has an open microporous structure. It is an improvement of an earlier reported hybrid membrane that contained non-bridging methylsilyl groups next to the organo-bridged silyl moieties. In addition, by optimizing the procedure, the recipe has undergone substantial simplification, which enables further tuning and development of this class of materials. While the average pore diameter has increased slightly with respect to the first generation hybrid silica membranes, this did not affect the selectivity in *n*-butanol dehydration. The material was found to be highly stable at 150 °C under hydrothermal conditions and membranes allowed continuous operation during at least one and a half years, without any decline of selectivity. The membrane showed step improvements in flux and perseverance thereof, compared to the previously reported membrane that also contained methylsilyl groups. Acid stability is high, even at acid concentrations equivalent to a pH of about 2. Only at higher acid concentrations, a decline of the flux was observed, combined with a selectivity decrease. The structure of this improved microporous hybrid silica material and its potential to coat very thin layers make it highly suitable for economical application in dehydration processes. Therefore, our current activities aim at defining the potentially very wide operation window of this new class of hybrid silica membranes.

References

[1] K. Keizer, R.J.R. Uhlhorn, R.J. Vanvuren, A.J. Burggraaf, Gas separation mechanisms in microporous modified gamma-Al₂O₃ membranes, J. Membr. Sci. 39 (1988) 285–300.
[2] R.M. de Vos, H. Verweij, High-selectivity, high-flux silica membranes for gas separation, Science 279 (1998) 1710–1711.
[3] R.M. de Vos, H. Verweij, Improved performance of silica membranes for gas separation, J. Membr. Sci. 143 (1998) 37–51.
[4] A. Tavolaro, E. Drioli, Zeolite membranes, Adv. Mater. 11 (1999) 975–996.
[5] T. Ban, T. Ohwaki, Y. Ohya, Y. Takahashi, Preparation of a completely oriented molecular sieve membrane, Angew. Chem. Intern. Ed. 38 (1999) 3324–3326.
[6] M.B. Shiflett, H.C. Foley, Ultrasonic deposition of high-selectivity nanoporous carbon membranes, Science 285 (1999) 1902–1905.
[7] L. Cot, A. Ayral, J. Durand, C. Guizard, N. Hovnanian, A. Julbe, A. Larbot, Inorganic membranes and solid state sciences, Solid State Sci. 2 (2000) 313–334.
[8] Z.P. Lai, G. Bonilla, I. Diaz, J.G. Nery, K. Sujaoti, M.A. Amat, E. Kokkoli, O. Terasaki, R.W. Thompson, M. Tsapatsis, D.G. Vlachos, Microstructural optimization of a zeolite membrane for organic vapor separation, Science 300 (2003) 456–460.
[9] M.C. Duke, J.C.D. da Costa, D.D. Do, P.G. Gray, G.Q. Lu, Hydrothermally robust molecular sieve silica for wet gas separation, Adv. Funct. Mater. 16 (2006) 1215–1220.
[10] L.M. Vane, A review of pervaporation for product recovery from biomass fermentation processes, J. Chem. Technol. Biotechnol. 80 (2005) 603–629.
[11] R.W. van Gemert, F.P. Cuperus, Newly developed ceramic membranes for dehydration and separation of organic mixtures by pervaporation, J. Membr. Sci. 105 (1995) 287–291.
[12] S. Sommer, T. Melin, Influence of operation parameters on the separation of mixtures by pervaporation and vapor permeation with inorganic membranes. Part 1. Dehydration of solvents, Chem. Eng. Sci. 60 (2005) 4509–4523.
[13] S. Sommer, T. Melin, Performance evaluation of microporous inorganic membranes in the dehydration of industrial solvents, Chem. Eng. Process. 44 (2005) 1138–1156.
[14] A.M. Urtiaga, E.D. Gorri, P. Gomez, C. Casado, R. Ibanez, I. Ortiz, Pervaporation technology for the dehydration of solvents and raw materials in the process industry, Drying Technol. 25 (2007) 1819–1828.
[15] S. Sommer, T. Melin, Design and optimization of hybrid separation processes for the dehydration of 2-propanol and other organics, Ind. Eng. Chem. Res. 43 (2004) 5248–5259.
[16] J.L. Humphrey, A.F. Seibert, Separation technologies—an opportunity for energy savings, Chem. Eng. Progress 88 (1992) 32–41.
[17] D.W. Breck, Zeolite Molecular Sieves: Structure, Chemistry, and Use, Wiley, New York, 1974.
[18] J.C.S. Wu, H. Sabol, G.W. Smith, D.L. Flowers, P.K.T. Liu, Characterization of hydrogen-permselective microporous ceramic membranes, J. Membr. Sci. 96 (1994) 275–287.
[19] S. Morooka, S. Yan, K. Kusakabe, Y. Akiyama, Formation of hydrogen-permselective SiO₂ membrane in macropores of alpha-alumina support tube by thermal decomposition of TEOS, J. Membr. Sci. 101 (1995) 89–98.
[20] A. Larbot, A. Julbe, C. Guizard, L. Cot, Silica membranes by the sol–gel process, J. Membr. Sci. 44 (1989) 289–303.
[21] R.K. Iler, The Chemistry of Silica, Wiley & Sons Inc., New York, USA, 1979.
[22] B.K. Sea, E. Soewito, M. Watanabe, K. Kusakabe, S. Morooka, S.S. Kim, Hydrogen recovery from a H₂–H₂O–HBr mixture utilizing silica-based membranes at elevated temperatures. 1. Preparation of H₂O- and H₂-selective membranes, Indust. Eng. Chem. Res. 37 (1998) 2502–2508.
[23] J. Campaniello, C.W.R. Engelen, W.G. Haije, P.P.A.C. Pex, J.F. Vente, Long-term pervaporation performance of microporous methylated silica membranes, Chem. Commun. (2004) 834–835.
[24] S.P. Nunes, K.V. Peinemann, Membrane Technology in the Chemical Industry, Wiley-VCH, Weinheim, 2001.
[25] A. Jonquieres, R. Clement, P. Lochon, J. Neel, M. Dresch, B. Chretien, Industrial state-of-the-art of pervaporation and vapour permeation in the western countries, J. Membr. Sci. 206 (2002) 87–117.
[26] R. Kreiter, C.W.R. Engelen, D.P. Wolfs, H.M. van Veen, J.F. Vente, High temperature pervaporation performance of ceramic-supported polyimide membranes in the dehydration of alcohols, J. Membr. Sci. 319 (2008) 126–132.
[27] M. Noack, P. Kolsch, R. Schafer, P. Toussaint, J. Caro, Molecular sieve membranes for industrial application: problems, progress, solutions (Reprinted from Chem. Ing. Tech. 73 (2001) 958–967), Chem. Eng. Technol. 25 (2002) 221–230.
[28] M. Asaeda, M. Kashimoto, Sol–gel derived silica membranes for separation of hydrogen at high temperature-separation performance and stability against steam, in: Proceedings of the Fifth International Conference on Inorganic Membranes, Nagoya, Japan, 1998, p. 172.
[29] H. Imai, H. Morimoto, A. Tominaga, H. Hirashima, Structural changes in sol–gel derived SiO₂ and TiO₂ films by exposure to water vapor, J. Sol–Gel Sci. Technol. 10 (1997) 45–54.

[30] R. Kreiter, M.D.A. Rietkerk, B.C. Bonekamp, H.M. van Veen, V.G. Kessler, J.F. Vente, Sol–gel routes towards microporous titania and zirconia membranes, J. Sol–Gel Sci. Technol. (2008), doi:10.1007/s10971-008-1760-x.

[31] G.I. Spijksma, C. Huiskes, N.E. Benes, H. Kruidhof, D.H.A. Blank, V.G. Kessler, H.J.M. Bouwmeester, Microporous zirconia–titania composite membranes derived from diethanolamine-modified precursors, Adv. Mater. 18 (2006) 2165–2168.

[32] G.P. Fotou, Y.S. Lin, S.E. Pratsinis, Hydrothermal stability of pure and modified microporous silica membranes, J. Mater. Sci. 30 (1995) 2803–2808.

[33] K. Yoshida, Y. Hirano, H. Fujii, T. Tsuru, M. Asaeda, Hydrothermal stability and performance of silica–zirconia membranes for hydrogen separation in hydrothermal conditions, J. Chem. Eng. Jpn. 34 (2001) 523–530.

[34] V. Boffa, D.H.A. Blank, J.E. ten Elshof, Hydrothermal stability of microporous silica and niobia–silica membranes, J. Membr. Sci. 319 (2008) 256–263.

[35] R.M. de Vos, W.F. Maier, H. Verweij, Hydrophobic silica membranes for gas separation, J. Membr. Sci. 158 (1999) 277–288.

[36] J.C.D. da Costa, G.Q. Lu, V. Rudolph, Characterisation of templated xerogels for molecular sieve application, Coll. Surf. A Physicochem. Eng. Aspects 179 (2001) 243–251.

[37] H.L. Castricum, A. Sah, R. Kreiter, D.H.A. Blank, J.F. Vente, J.E. ten Elshof, Hybrid ceramic nanosieves: stabilizing nanopores with organic links, Chem. Commun. (2008) 1103–1105.

[38] H.L. Castricum, A. Sah, R. Kreiter, D.H.A. Blank, J.F. Vente, J.E. ten Elshof, Hydrothermally stable molecular separation membranes from organically linked silica, J. Mater. Chem. 18 (2008) 2150–2158.

[39] D.A. Loy, K.J. Shea, Bridged polysilsesquioxanes—highly porous hybrid organic–inorganic materials, Chem. Rev. 95 (1995) 1431–1442.

[40] K.J. Shea, D.A. Loy, Bridged polysilsesquioxanes. Molecular-engineered hybrid organic–inorganic materials, Chem. Mater. 13 (2001) 3306–3319.

[41] K.J. Shea, D.A. Loy, A mechanistic investigation of gelation. The sol–gel polymerization of precursors to bridged polysilsesquioxanes, Acc. Chem. Res. 34 (2001) 707–716.

[42] T. Asefa, M.J. MacLachlan, N. Coombs, G.A. Ozin, Periodic mesoporous organosilicas with organic groups inside the channel walls, Nature 402 (1999) 867–871.

[43] J. Alauzun, A. Mehdi, C. Reye, R.J.P. Corriu, Mesoporous materials with an acidic framework and basic pores. A successful cohabitation, J. Am. Chem. Soc. 128 (2006) 8718–8719.

[44] F. Hoffmann, M. Cornelius, J. Morell, M. Froba, Silica-based mesoporous organic–inorganic hybrid materials, Angew. Chem. Intern. Ed. 45 (2006) 3216–3251.

[45] B.C. Bonekamp, Preparation of asymmetric ceramic membrane supports by dip-coating, in: A.J. Burggraaf, L. Cot (Eds.), Fundamentals of Inorganic Membrane Science and Technology, vol. 4, Elsevier, Amsterdam, The Netherlands, 1996, pp. 141–221 (Chapter 6).

[46] H.M. van Veen, Y.C. van Delft, C.W.R. Engelen, P.P.A.C. Pex, Dewatering of organics by pervaporation with silica membranes, Sep. Purif. Technol. 22/23 (2001) 361–366.

[47] F.T. Rusting, G. de Jong, P.P.A.C. Pex, J.A.J. Peters, Sealing socket and method for arranging a sealing socket to a tube, International Patent WO 01/63162A1 (2001).

[48] W. Bras, I.P. Dolbnya, D. Detollenaere, R. vanTol, M. Malfois, G.N. Greaves, A.J. Ryan, E. Heeley, Recent experiments on a combined small-angle/wide-angle X-ray scattering beam line at the ESRF, J. Appl. Crystallogr. 36 (2003) 791–794.

[49] M.G. Kaganer, A new method for the determination of the specific adsorption surface of adsorbents and other finely dispersed substances, Zh. Fiz. Khim. 33 (1959) 2202–2210.

[50] S.J. Gregg, K.S.W. Sing, Adsorption, Surface Area and Porosity, Academic Press, London, UK, 1982.

[51] T. Tsuru, T. Hino, T. Yoshioka, M. Asaeda, Permporometry characterization of microporous ceramic membranes, J. Membr. Sci. 186 (2001) 257–265.

[52] H.W. Deckman, R.R. Chance, D.M. Cox, W.G. deGijnst, J.J. Reinoso, Characterization of membranes, United States Patent US 2003/0005750 (2003).

[53] H.L. Castricum, A. Sah, J.A.J. Geenevasen, R. Kreiter, D.H.A. Blank, J.F. Vente, J.E. ten Elshof, Structure of hybrid organic–inorganic sols for the preparation of hydrothermally stable membranes, J. Sol–Gel Sci. Technol. (2008), doi:10.1007/s10971-008-1742-z.

[54] C.J. Brinker, G.C. Frye, A.J. Hurd, C.S. Ashley, Fundamentals of sol–gel dip coating, Thin Solid Films 201 (1991) 97–108.

[55] R.S.A. de Lange, J.H.A. Hekkink, K. Keizer, A.J. Burggraaf, Formation and characterization of supported microporous ceramic membranes prepared by sol–gel modification techniques, J. Membr. Sci. 99 (1995) 57–75.

[56] M.M. Dubinin, On physical feasibility of Brunauer's micropore analysis method, J. Colloid Interf. Sci. 46 (1974) 351–356.

[57] M.C. Mittelmeijer-Hazeleger, H. De Jonge, A. Bliek, Determination of the surface area and pore sizes of organic matter in soils, in: B. McEnaney, T.J. Mays, J. Rouquérol, F. Rodriguez-Reinoso, K.S.W. Sing, K.K. Unger (Eds.), Characterization of Porous Solids IV, Royal Soc. Chem., Cambridge, UK, 1996, pp. 429–436.

[58] H.L. Castricum, A. Sah, M.C. Mittelmeijer-Hazeleger, C. Huiskes, J.E. ten Elshof, Microporous structure and enhanced hydrophobicity in methylated SiO_2 for molecular separation, J. Mater. Chem. 17 (2007) 1509–1517.